2008

In vivo strains in the femur of river cooter turtles (Pseudemys concinna) during terrestrial locomotion: tests of force-platform models of loading mechanics

Michael T. Butcher

Nora R. Espinoza

Stephanie R. Cirilo

Richard W. Blob
Clemson University, rblob@clemson.edu

The Journal of Experimental Biology 211, 2397-2407
Published by The Company of Biologists 2008
doi:10.1242/jeb.018986

In vivo strains in the femur of river cooter turtles (*Pseudemys concinna*) during terrestrial locomotion: tests of force-platform models of loading mechanics

Michael T. Butcher[1], Nora R. Espinoza[1,2], Stephanie R. Cirilo[2] and Richard W. Blob[1,*]

[1]Department of Biological Sciences, Clemson University, Clemson, SC 29634, USA and [2]Department of Biology, Erskine College, Due West, SC 29639, USA

*Author for correspondence (e-mail: rblob@clemson.edu)

Accepted 15 May 2008

SUMMARY

Previous analyses of ground reaction force (GRF) and kinematic data from river cooter turtles (*Pseudemys concinna*) during terrestrial walking led to three primary conclusions about the mechanics of limb bone loading in this lineage: (1) the femur was loaded in a combination of axial compression, bending and torsion, similar to previously studied non-avian reptiles, (2) femoral shear stresses were high despite the possession of a reduced tail in turtles that does not drag on the ground and (3) stress-based calculations of femoral safety factors indicated high values in bending and torsion, similar to other reptiles and suggesting that substantial 'overbuilding' of limb bones could be an ancestral feature of tetrapods. Because force-platform analyses produce indirect estimates of bone loading, we sought to validate these conclusions by surgically implanting strain gauges on turtle femora to directly measure *in vivo* strains during terrestrial walking. Strain analyses verified axial compression and bending as well as high torsion in turtle femora, with peak axial strains comparable to those of other non-avian reptiles at similar walking speeds but higher peak shear strains approaching 2000 με. Planar strain analyses showed patterns of neutral axis (NA) of femoral bending orientations and shifting generally consistent with our previous force-platform analyses of bone stresses, tending to place the anterior and dorsal aspects of the femur in tension and verifying an unexpected pattern from our force studies that differs from patterns in other non-avian reptiles. Calculated femoral safety factors were 3.8 in torsion and ranged from 4.4 to 6.9 in bending. Although these safety factors in bending were lower than values derived from our stress-based calculations, they are similar to strain-based safety factors calculated for other non-avian reptiles in terrestrial locomotion and are still high compared with safety factors calculated for limb bones of birds and mammals. These findings are consistent with conclusions drawn from our previous models of limb bone stresses in turtles and suggest that not only are turtle limb bones 'overbuilt' in terms of resisting the loads that they experience during locomotion but also, across tetrapod lineages, elevated torsion and high limb bone safety factors may be primitive features of limb bone design.

Key words: locomotion, biomechanics, bone strain, safety factor, turtle.

INTRODUCTION

The morphology and structural design of tetrapod limb bones shows striking diversity. Because one of the primary functions of the skeleton is to resist and transfer mechanical loads, one of the main factors to which the diversity of limb bone designs has been attributed is variation in the loads that different species encounter (Currey, 1984; Bertram and Biewener, 1988; Blob, 2001; Currey, 2002; Lieberman et al., 2004; de Margerie et al., 2005). Among terrestrial tetrapods, the activity typically thought to impose the most frequent and severe loads on limb bones is locomotion (Biewener, 1990; Biewener, 1993). However, while the demands of locomotion may exert one of the greatest influences on the loading environments that limb bones experience, the loads that locomotion imposes on limb bones have been evaluated only from a limited functional and phylogenetic range of species. In particular, most limb bone loading data have been derived from birds and mammals (Rubin and Lanyon, 1982; Biewener, 1983a; Biewener, 1983b; Biewener et al., 1983; Biewener et al., 1988; Carrano, 1998; Demes et al., 2001; Lieberman et al., 2004; Main and Biewener, 2004; Main and Biewener, 2007), groups that both use predominantly parasagittal limb movements during locomotion (Jenkins, 1971; Carrano, 1998; Gatesy, 1999; Reilly, 2000). Considerably fewer studies have evaluated patterns of limb bone loading in species that use non-parasagittal limb kinematics (Blob and Biewener, 1999; Blob and Biewener, 2001; Butcher and Blob, 2008), such as reptile or amphibian taxa that employ a sprawling limb posture in which the limbs are held lateral to the body and the upper limb segments experience substantial axial rotation (Walker, 1971; Brinkman, 1980; Brinkman, 1981; Gatesy, 1991; Ashley-Ross, 1994a; Ashley-Ross, 1994b; Ashley-Ross, 1995; Reilly and Elias, 1998). Because differences in limb posture can affect the orientation of limb bones to the ground reaction force (GRF), thereby affecting bone loading (Biewener, 1983a; Biewener et al., 1983; Biewener et al., 1988; Blob and Biewener, 2001; Butcher and Blob, 2008), data on limb bone loading from species using non-parasagittal kinematics are critical for understanding correlations between limb bone loading and design throughout the evolution of tetrapods.

Although studies of terrestrial limb bone loading in non-parasagittal lineages have been limited, data from the hindlimbs of American alligators (*Alligator mississippiensis*, a crocodilian) and green iguanas (*Iguana iguana*, a lizard) during locomotion showed several common features (Blob and Biewener, 1999; Blob and Biewener, 2001). These included (1) moderate magnitudes of axial compression and bending during locomotion, with the primary

bending axis placing the anatomical anteroventral aspect of the femur in tension and more dorsoposterior aspects in compression; (2) considerable torsional loading, consistent with axial rotation of the femur during locomotion; and (3) high limb bone safety factors in both bending and shear. These findings contrasted with loading patterns and mechanical properties from limb bone loading studies of birds and mammals in two major ways. First, although torsion has been measured in the hindlimb bones of bipedal birds (Carrano, 1998; Main and Biewener, 2007), it is generally uncommon among quadrupedal mammals, in which bending and axial compression typically predominate (Biewener, 1990; Biewener, 1991) (although see Keller and Spengler, 1989). Second, due to higher functional bone loads during locomotion, the margin of safety for limb bones of birds and mammals is typically between 2 and 4 (Alexander, 1981; Biewener, 1993), as low as half that determined for non-avian reptilian lineages (Blob and Biewener, 1999; Blob and Biewener, 2001). Such differences might reflect adaptations of these lineages to differing demands; for example, high safety factors in reptiles might help to accommodate lower rates of bone remodeling or higher load variability than are found in birds or mammals (Blob and Biewener, 1999; Blob and Biewener, 2001). Alternatively, the loading patterns observed in alligators and iguanas might represent retained ancestral conditions from which birds and mammals independently diverged (Blob and Biewener, 1999; Blob and Biewener, 2001). However, with data only available from such a small number of non-avian reptilian species, it is unclear whether loading patterns from alligators and iguanas could be considered representative for non-avian reptiles more broadly and, thus, difficult to evaluate if they represent unique adaptations or ancestral retentions.

To broaden the phylogenetic and functional diversity of lineages in which limb bone loading patterns have been evaluated, and thereby gain better perspective on the evolution of tetrapod limb bone design, we recently calculated femoral stresses during terrestrial locomotion in river cooter turtles (*Pseudemys concinna*) based on three-dimensional GRF and kinematic data (Butcher and Blob, 2008). Not only do turtles represent an additional reptilian (*sensu* Modesto and Anderson, 2004) clade that could indicate whether the loading patterns of alligators and iguanas are restricted to their respective lineages, but also several distinctive features of turtles generated alternative, testable hypotheses for how the limb bones of this clade might be loaded in terrestrial locomotion (Butcher and Blob, 2008). For example, the slow walking speeds typical of turtles (Walker, 1971; Zug, 1971; Jayes and Alexander, 1980; Claussen et al., 2004) suggested that their limb bone loads might be low; however, their highly sprawled limb posture (Walker, 1971; Zug, 1971; Blob et al., 2008) would orient the limb at a large angle to the GRF, suggesting an alternative possibility of elevated bending loads (Biewener, 1989; Biewener, 1990). In addition, the sprawling limb posture of turtles suggested the potential for high torsion in their limb bones (Blob and Biewener, 1999; Blob and Biewener, 2001); however, recent studies proposing that limb bone torsion was primarily a consequence of dragging a heavy tail during locomotion (Willey et al., 2004; Reilly et al., 2005) suggested an alternative possibility that turtles might experience low limb bone torsion, as the tail is reduced and carried off the ground in most species (Willey and Blob, 2004). Our GRF-based analyses of limb bone loading in *P. concinna* (Butcher and Blob, 2008) indicated that femoral bending stress magnitudes in turtles were similar to those of other reptiles studied (Blob and Biewener, 2001) leading to similarly high bending safety factors. However, greater axial rotation of the femur during the step in cooters oriented the neutral axis of bending such that the anterodorsal aspect of the femur was placed in tension (Butcher and Blob, 2008), rather than the anteroventral aspect as observed in other reptiles (Blob and Biewener, 1999; Blob and Biewener, 2001). In addition, shear stresses in cooter femora were among the highest reported for any tetrapod limb bones during terrestrial locomotion, leading to torsional safety factors that were moderately lower than those calculated for alligators and iguanas, but still higher than those typical for birds and mammals (Butcher and Blob, 2008) (Butcher and Blob, in press). Thus, femoral loading in turtles appears more similar in most respects (e.g. magnitudes, regimes) to that observed in other non-avian reptiles compared to that observed in birds or mammals. However, femoral loading in turtles may still be distinctive from that of other tetrapods in some respects, such as the orientation of bending and the high degree of torsion.

Although our analysis of synchronized force-platform and kinematic data from cooters gave insight into the mechanics underlying their femoral loading through GRF data and estimates of limb muscle forces (Butcher and Blob, 2008), the force-kinematic approach to evaluating bone loads has important limitations (Biewener et al., 1983; Biewener and Full, 1992). Foremost, force-platform data generate indirect estimates of load magnitudes *via* calculations requiring several assumptions, particularly regarding the actions of limb muscles (Alexander, 1974; Biewener and Full, 1992; Blob and Biewener, 2001; Butcher and Blob, 2008). In some cases, such as for the forces exerted by caudofemoral muscles to rotate the femur about its long axis (Blob and Biewener, 2001; Butcher and Blob, 2008), an insufficient basis is available for making assumptions about muscular contributions to bone loading, and only minimum estimates of load magnitudes (due to the GRF alone) can be calculated. With such limitations, direct *in vivo* measurements of limb bone loads can provide an important means of verifying conclusions derived from force-kinematic models of bone loading.

This study reports results of *in vivo* locomotor strain recordings from the femur of river cooter turtles during terrestrial locomotion. Although implanted strain gauges do not give specific insight into the forces underlying bone loading patterns, direct measurements of femoral strains test the validity of the loading patterns inferred from models based on GRF and kinematic data and allow direct comparison with a wide range of studies in which bone loading mechanics have been evaluated *via* direct strain recordings (e.g. Rubin and Lanyon, 1982; Biewener et al., 1983; Nunamaker et al., 1990; Davies et al., 1993; Blob and Biewener, 1999; Demes et al., 2001; Main and Biewener, 2004; Main and Biewener, 2007). Strain data are also particularly amenable to analyses of loading rates (Ross et al., 2007), providing an additional method for assessing differences in bone mechanics across species. Based on our force-platform analyses of femoral stresses in cooters (Butcher and Blob, 2008) and *in vivo* femoral strains recorded from other reptiles (Blob and Biewener, 1999), we hypothesized that the femur of cooters would experience high magnitudes of shear strain, indicating that torsional loading is not exclusive to animals that drag a large tail (Reilly et al., 2005) and may be a fundamental mechanical consequence of sprawling limb posture. We further hypothesized that *in vivo* strains experienced by the femur in river cooters would be similar to or (in the case of shear strains) higher than those measured for other non-avian reptiles but that femoral safety factors for cooters, like those for other reptiles, would be substantially higher than those calculated for birds and mammals. Thus, our measurements of limb bone strains from cooter femora provide an independent means of verifying interpretations of limb bone loading in turtles based on force-platform analyses, facilitating evaluations of the diversity of tetrapod limb bone design.

MATERIALS AND METHODS

Animals

Six river cooter turtles, *Pseudemys concinna* (LeConte), were used in experiments, including three used in our previous analyses of locomotor GRFs and bone stresses (Butcher and Blob, 2008). Cooters (0.82–3.95 kg body mass; one sub-adult male, one adult male and four adult females) were collected from a spillway of Lake Hartwell (Pickens County, SC, USA) and housed in a greenhouse in large plastic cattle tanks or mixing tubs half-filled with fresh water and fitted with re-circulating filters and dry basking ramps. Turtles were fed daily (collard or turnip greens supplemented with commercial pellets) and exposed to ambient light conditions. For approximately 2–4 weeks prior to experiments, turtles were trained to walk on a motorized treadmill (model DC5; Jog A Dog®, Ottawa Lake, MI, USA) involving 5–10 min bouts of walking at moderate speed several times weekly.

Surgical procedures

Strain gauges were attached surgically to the right femur of each animal using aseptic technique and following published methods (Biewener, 1992; Blob and Biewener, 1999). All surgical and experimental procedures followed protocols approved by the Clemson University IACUC (AUP 20030 and 50110). Initial doses of 1 mg kg^{-1} butorphenol and 100 mg kg^{-1} ketamine were injected into the forelimb musculature to induce analgesia and a surgical plane of anesthesia, with supplemental doses administered as required.

To expose strain-gauge attachment sites, medial incisions were made through the skin on the anteroventral aspect of the thigh at mid-shaft. Muscles surrounding the femur were separated along the fascial plane between the ambiens and pubotibialis, which were retracted to gain access to the bone. Gauges were attached at mid-shaft, or slightly distal to mid-shaft if necessary to avoid disruption of blood vessels or attachments of the femorotibialis muscle reaching around from the dorsal surface of the bone. At the site where gauges were to be attached, a 'window' of periosteum was removed to expose the bone cortex. Bone surfaces were gently scraped with a periosteal elevator, swabbed clean with ether using a cotton-tipped applicator and allowed to dry for several seconds. Gauges were then attached using a self-catalyzing cyanoacrylate adhesive (Duro™ Superglue; Henkel Loctite Corp., Avon, OH, USA).

Single element (SE) and rosette (ROS) strain gauges (type FLG-1-11 and FRA-1-11, respectively; Tokyo Sokki Kenkyujo, Japan) were attached to surfaces of the femur designated as 'dorsal', 'anterior' and 'ventral', following conventions of anatomical orientation established for reptiles by Romer (Romer, 1956) and illustrated in our previous analysis of femoral stresses in cooters (see fig. 1 in Butcher and Blob, 2008). The size of the femora in our animals allowed only one ROS gauge, at most, to be used in each individual. Locations of ROS placement varied across our individuals depending on the access available in each animal, but this allowed us to attach a ROS gauge to each targeted anatomical surface over the course of all experiments (dorsal surface for individuals pc03 and pc05, anterior surface for pc04, and ventral surface for pc07). In most individuals, SE gauges were attached to both of the two target bone surfaces remaining after placement of the ROS. SE and the central elements of ROS were aligned (within 5°) with the long axis of the femur. Once all gauges were in place, lead wires from the gauges (336 FTE, etched Teflon; Measurements Group, Raleigh, NC, USA) were passed subcutaneously though a small, proximal skin incision on the posterodorsal aspect of the thigh (near the hip) and, additionally, through a small hole drilled through the posterior margin of the carapace, after which all incisions were sutured closed. Lead wires were then soldered into a microconnector and secured (with slack) to the shell by tying the wires into the carapace hole with suture. Solder connections were reinforced with epoxy adhesive, and self-adhesive bandage was wrapped around exposed portions of the lead wires to form a protective cable that was secured to the shell with tape.

In vivo strain data collection and data analysis

After 1–2 days of recovery, *in vivo* strain recordings were made over the following 2 days. Strain signals were conducted from the gauges to Vishay conditioning bridge amplifiers (model 2120B; Measurements Group) *via* a shielded cable. Raw voltage signals from strain gauges were sampled through an A/D converter (model PCI-6031E; National Instruments Corp., Austin, TX, USA) at 2500 Hz, saved to computer using data acquisition software written in LabVIEW™ (v. 6.1; National Instruments) and calibrated to microstrain ($\mu\varepsilon$=strain$\times10^{-6}$). Strain data were collected while animals walked on the motorized treadmill used for locomotor training. Most recordings consisted of short trials of moderate (0.05–0.15 m s^{-1}; 0.2–0.6 carapace lengths s^{-1}), steady-speed walking with data sampled from 4–8 consecutive footfalls of the right hindlimb. In general, the speeds achieved by each turtle required considerable exertion and were close to the maximal speed that it could sustain for 3–4 steps. Periods of rest were given between trials, and temperature within the treadmill enclosure was maintained near or above 25°C by heat lamps for all trials.

To document locomotor behavior and footfall patterns during strain trials, lateral- and posterior-view high-speed (100 Hz) video data (Phantom V4.1; Vision Research Inc., Wayne, NJ, USA) of locomotion were collected. Video data were synchronized with strain recordings using an LED visible in the camera frames that simultaneously produced 1.5 V pulses visible in strain records. Upon completion of strain recordings, animals were killed by an overdose of a pentobarbital sodium solution (Euthasol®; Delmarva Laboratories Inc., Midlothian, VA, USA; 200 mg kg^{-1} intraperitoneal injection) and frozen for later dissection, verification of gauge placement and limb bone mechanical property tests.

Standard conventions for analysis and interpretation of strain data were employed, following our previous studies of non-avian reptile limb bone loading (Blob and Biewener, 1999). Briefly, tensile strains are recorded as positive, and compressive strains are negative. The magnitudes of peak axial strains (aligned with the long axis of the femur) were determined from each gauge location for each step of the right hindlimb. Strain magnitudes were evaluated for N=10–80 steps from each cooter (depending on quality of recordings from each individual). The distribution of tensile and compressive strains on the cortex of the femur was then used to evaluate the loading regime the bone experienced during locomotion. For instance, equal magnitudes of tensile and compressive strain on opposite cortices would indicate pure bending, whereas unequal magnitudes of tension and compression on opposite cortices would indicate a combination of axial and bending loads. Magnitudes and orientations of peak principal strains (i.e. maximum and minimum strains at each site, regardless of alignment with the femoral long axis), as well as shear strain magnitudes, were calculated from ROS data following published methods (Carter, 1978; Dally and Riley, 1978; Biewener and Dial, 1995). Determination of principal strain orientations and shear strain magnitudes allowed evaluation of the importance of torsional loading in cooter femora. Defining the long axis of the femur as 0°, pure torsional loads would show principal

strain orientations (deviations from the bone long axis) of 45° or –45°, respectively, depending on whether the femur was twisted in a clockwise or counterclockwise direction. Orientations of principal tensile strain (ϕ_t) differing by 180° are equivalent, and orientations of peak principal tensile and compressive strains are orthogonal.

Following muscular dissections of the hindlimbs of the animals (Butcher and Blob, 2008), instrumented femora were excised, swabbed clean of tissue and embedded in fiberglass resin. Transverse sections were cut from each embedded femur through the mid-shaft gauge locations, and one cross-section from each femur was then photographed using a digital camera mounted on a dissecting microscope. Microsoft Powerpoint was used to trace endosteal and periosteal outlines of the cross-sections from the photographs, mark locations of the three gauges on the bone perimeter and save cross-sectional tracings as JPEG files. Each bone's geometric data were then input along with strain data from its three femoral gauge locations into analysis macros for the public domain software NIH Image for Macintosh (http://rsb.info.nih.gov/nih-image/) in order to calculate the location of the neutral axis (NA) of bending and the planar distribution of longitudinal strains through femoral cross sections (Lieberman et al., 2003; Lieberman et al., 2004). Planar strain analyses were conducted on a subset of data (N=50 steps), allowing calculation of peak values of tensile and compressive strain that may have occurred at locations other than recording sites (Carter et al., 1981; Biewener and Dial, 1995). Calculated peak strains were then compared to measured peak strains to determine the proportional increase in strain between the recorded peaks and calculated peak magnitudes. Additionally, in a subset of these data (N=18; 6 steps per individual), planar strain distributions were calculated at five time points during a step (15%, 30%, 50%, 70% and 85% of contact) to evaluate shifts in the location and orientation of the NA throughout the step.

Rates of longitudinal strain were also determined for a sub-sample of steps (N=60 steps, two individuals) by calculating slopes of linear, least-squares regressions of strain magnitude on time during the loading portion of footfalls. Measurements of peak strain rate from the 'dorsal' gauge location were used to determine rates of strain for mechanical property testing of the limb bones. Strain magnitudes were also regressed on strain rates from corresponding steps to evaluate the relationship between load rate and magnitude for turtle femora (Ross et al., 2007).

Mechanical properties and safety factors

Yield strains were evaluated in three-point bending and torsion for intact cooter limb bones that were not instrumented during *in vivo* strain recording trials. Details of testing procedures were described previously in the context of reporting yield stress values (Butcher and Blob, 2008) and are only briefly summarized here. For bending tests (model 4502 uniaxial testing machine with 10 kN load cell; Instron, Norwood, MA, USA), whole bones (N=3 femora, 4 tibiae) were mounted in the jig (0.025 or 0.030 m gauge length) so that the dorsal-to-anterodorsal (femur) or anterior (tibia) surface was loaded in tension, consistent with patterns from *in vivo* strain recordings (for the femur, see below) and providing a stable seating that accommodated the natural curvature of the bones. Cortical bone strains were recorded during tests using three SE gauges attached to the mid-shaft (Blob and Biewener, 1999). For femora, gauges were mounted on the anterior, anterodorsal and posterodorsal surfaces; for tibiae, gauges were mounted on the anterior, medial and lateral surfaces. Strain gauge signals were amplified, sampled (500 Hz) through an A/D converter in LabVIEW and calibrated as detailed previously. Applied load and displacement data were sampled at 10 Hz until failure, and crosshead displacement rate was set at 4.5 mm m^{-1}, based on strain rate measurements (Cirilo et al., 2005). Separate whole bone specimens (N=3 femora) were used for torsional tests (model 8874 biaxial testing machine with 25 kN load cell; Instron, Norwood, MA, USA) by attaching two ROS gauges to the mid-shaft of each bone (dorsal and ventral surfaces). Bones were suspended in machined aluminum wells into which epoxy was poured to embed 15 mm of the ends of each bone. Once hardened, embedded ends were fitted into mounting brackets in the testing jig and twisted to failure. Twisting rate was set at 3 ° s^{-1} (Furman and Saha, 2000) and performed in a direction to simulate *in vivo* anterior (i.e. inward) rotation.

Yield point was identified from plots of applied bending (or twisting) moment *versus* maximum tensile (or shear) strain as the first point where measured strain magnitude deviated from the magnitude expected based on the initial, linear slope of the curve by 200 με (Currey, 1990). Safety factors for the femur of *P. concinna* were calculated as the ratio of yield strain to peak locomotor strains (based on tensile loads for femoral bending and shear loads for femoral torsion). Safety factors were first calculated for each individual from the mean values of peak locomotor strains (principal and shear strains) multiplied by a proportional value of strain increase determined from planar strain distribution analyses (Blob and Biewener, 1999). 'Mean' safety factors were then calculated as the grand mean of safety factors for these individuals. 'Worst case' safety factors in bending and shear were calculated using the single highest value of recorded peak tensile strain and shear strain, respectively, after adjusting for the proportional increase in strain estimated based on planar strain analyses.

RESULTS

Locomotor strain patterns and magnitudes

Generalizations about limb bone strains in cooters during walking were made on the basis of the most common strain patterns observed for each recording site, interpreting these patterns as standard behavior. Peak strain magnitudes were variable among the six individual turtles (coefficients of variation averaged 34.4% across all gauge locations). Also, because of minor differences in gauge placement among individuals, some gauge locations (particularly those determined by planar strain analyses to be near the NA, such as the ventral location) showed variable patterns among individuals as to whether peak strains were tensile or compressive. However, patterns of tensile and compressive strain at each recording location were generally consistent between steps for a given individual, allowing a general interpretation of femoral loading in cooters to be developed.

Representative patterns of recorded strains are shown in Fig. 1. Peak axial and principal strains at all gauge locations were nearly synchronous and typically occurred before midstance (25–48% of contact), with the exception of axial strains at the ventral site. Ventral axial strain records consistently showed lower peak magnitudes than other sites (Table 1) and frequently showed two peaks per step, with low magnitudes between these peaks occurring near the time of peak axial and principal strains at other gauge locations (Fig. 1). Principal (and shear) strain traces typically showed only single peaks, similar to observations during vigorous locomotion in other species ranging from reptiles (Blob and Biewener, 1999) to mammals (Rubin and Lanyon, 1982; Biewener and Taylor, 1986; Main and Biewener, 2004).

Strain distributions and the relative magnitudes of tension and compression around the cortex indicate that the cooter femur is loaded in a combination of axial compression and bending. Dorsal

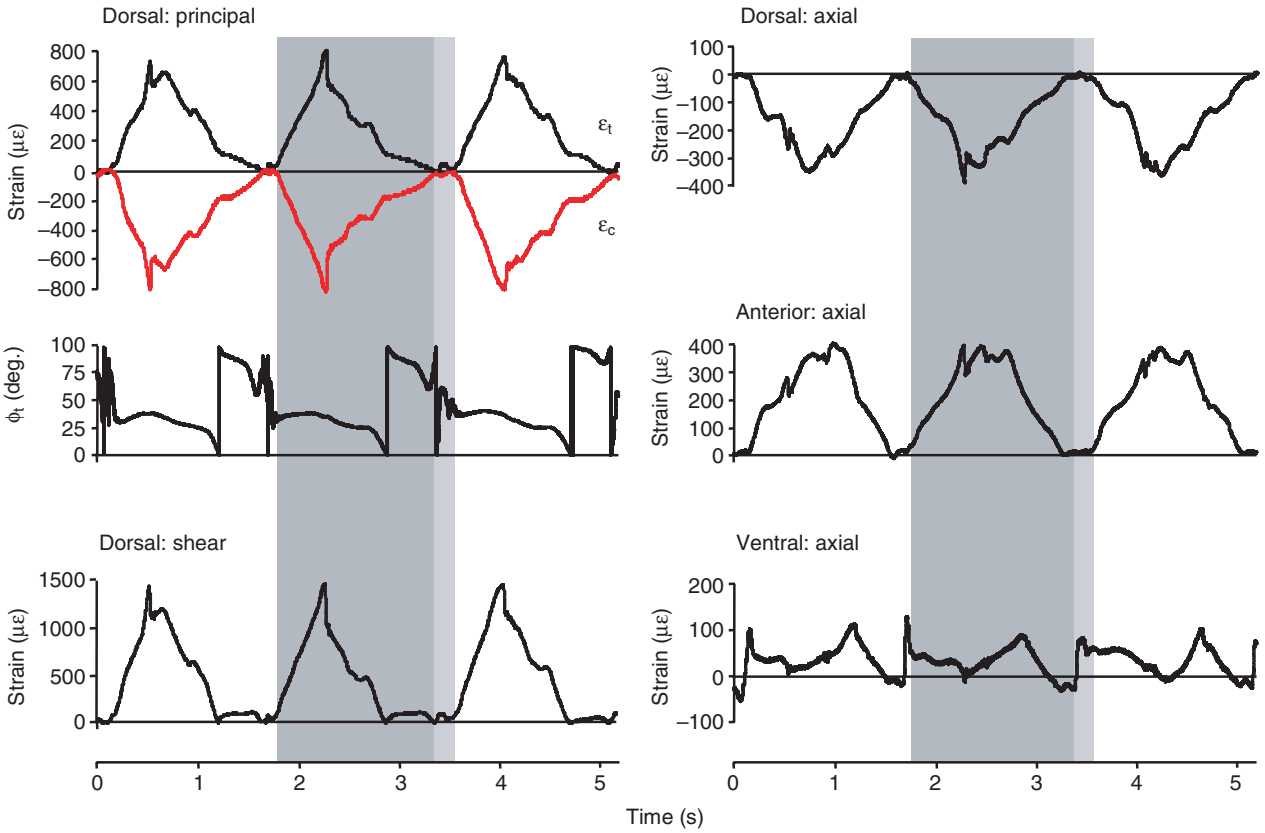

Fig. 1. Representative strain recordings (simultaneous) from three gauge locations on the cooter femur during three consecutive walking steps. Left: principal strains, angle of principal tensile strains from the femoral long axis (ϕ_t) and shear strains from ROS gauge recordings. Right: longitudinal strains from 'dorsal', 'anterior' and 'ventral' sites. Note that strain scales differ among panels to facilitate presentation. Dark gray shading highlights the stance phase (contact) for a single step at all gauge locations. Light gray shading highlights the swing phase of a stride. ε_t and ε_c denote tensile and compressive (red line) principal strain traces, respectively.

and ventral recording locations on cooter femora typically experienced compression (Table 1). Peak axial strains were generally negative at these sites, and compressive principal strains were greater in magnitude than tensile principal strains at these locations (Table 1). By contrast, tensile strains appeared to predominate at the anterior recording location. Although ROS data from an anterior gauge in a single individual showed a higher magnitude of peak compressive principal strain than peak tensile principal strain, average strains across five individuals showed peak axial strains that were generally tensile (Table 1). The presence of tensile strains on the anterior surface and compressive strains on the dorsal and ventral surfaces indicates that the cooter femur is loaded in bending. Furthermore, because compressive axial strains on the dorsal surface were, on average, greater in magnitude than tensile axial strains on the anterior surface, femoral bending appears to be superimposed on axial compression related to supporting the weight of the body.

In addition to bending and axial compression, strain data show that cooter femora are also exposed to substantial torsion. Average ϕ_t on the dorsal, anterior and ventral surfaces of the femur all deviated strongly from the long axis of the bone, with values (typically 41–51°) near the 45° value expected for torsional loading (Table 1, Fig. 1). Based on conventions for gauge configurations in our experiments, positive mean values for ϕ_t indicated anterior (i.e. inward) rotation of the femur during the step. This direction of rotation is consistent with expectations based on the action of the femoral retractor/rotator muscle caudi-iliofemoralis in turtles (Walker, 1973), as well as the torsional moments induced by the net GRF (Butcher and Blob, 2008). High magnitudes of peak shear strains further indicate substantial torsional loading of cooter femora

Table 1. Peak axial (ε_{axial}), principal tensile (ε_t), principal compressive (ε_c) and shear strains recorded from the river cooter (*Pseudemys concinna*) femur during walking

Gauge location	ε_{axial} (με)	ε_t (με)	ε_c (με)	ϕ_t (deg.)	Shear (με)
Dorsal	–486.2±593.9 (255, 5)	715.7±11.5 (74, 2)	–825.9±125.5 (74, 2)	50.3±8.9 (74, 2)	1441.3±109.7 (74, 2)
Anterior	218.9±118.2 (242, 5)	1310.2±188.5 (81, 1)	–1701.2±212.1 (81, 1)	42.6±2.1 (81, 1)	2934.9±407.8 (81, 1)
Ventral	–104.5±49.7 (263, 6)	833.4±189.7 (76, 1)	–975.7±189.4 (76, 1)	41.2±2.7 (76, 1)	1788.1±372.4 (76, 1)
Mean ± s.d.	–	893.7±283.2	–1082.2±424.9	46.1±7.1	1901.4±711.0

Values are means (± s.d.) across all individuals. In parentheses are the number of steps analyzed and the number of individuals tested, respectively.
Angles of principal tensile strains to the long axis of the bone (ϕ_t) are also reported. Positive angles for ϕ_t indicate inward (anterior) rotation for all gauge locations.

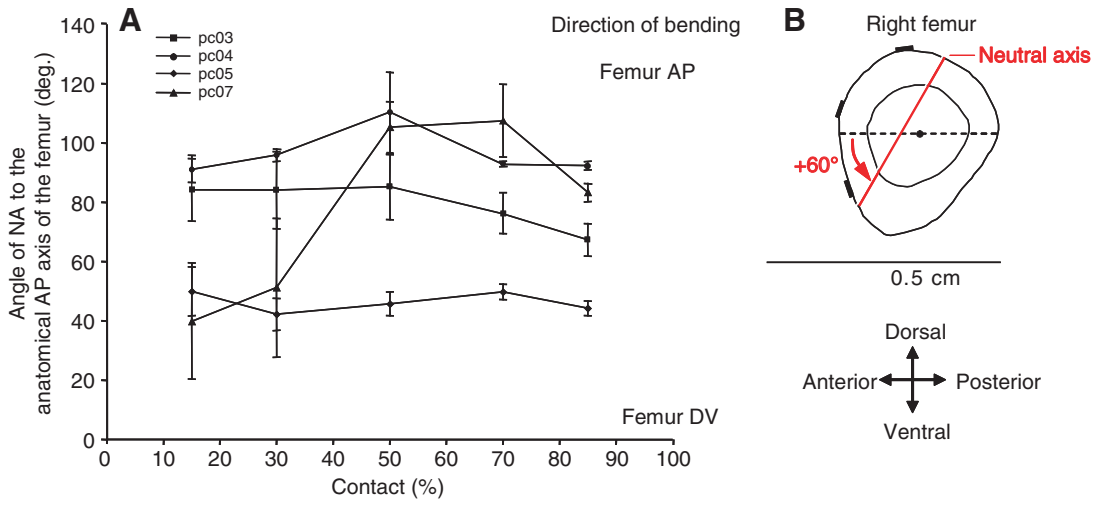

Fig. 2. (A) Shifts in the orientation of the neutral axis (NA) of femoral bending at five time increments (% of contact) through the step for four individual cooters. Each data point represents the angle of the NA to the anatomical anteroposterior (AP) axis of the femur averaged over *N*=3–6 steps. (B) Schematic femur cross section illustrating NA orientation and shift. Strain gauge locations are indicated by the black bars around the cortex of the femoral cross-section. Solid red line is an NA with an orientation of 60°. Directions of bending are indicated with respect to the anatomical axes of the bone as described in the text, not in an absolute frame of reference. AP, bending about an NA running from the anatomical dorsal to ventral cortex; DV, bending about an NA running from the anatomical anterior to posterior cortex.

(Table 1). Peak shear strains were particularly high for the one individual (pc04) in which they were recorded from the anterior location, averaging 2934.9±407.8 με (Table 1). However, shear strains were also high on the dorsal and ventral surfaces of the femur (>1400 με on average), markedly exceeding values reported for the same surfaces of the femur in alligators and iguanas during running (Blob and Biewener, 1999). Femoral shear strains exceeded average peak principal strain measurements (compressive) from the dorsal, anterior and ventral gauge locations by 74%, 73% and 83%, respectively (Table 1, Fig. 1).

Planar strain distribution analyses and neutral axis orientation

Planar strain analyses showed similar patterns for most individuals through most of stance phase, although some cases of individual variation were evident. At the beginning of the step, the NA was typically aligned diagonally between the anatomical AP and DV axes and shifted anterior and slightly dorsal from the cross-sectional centroid (Figs 2, 3), with only anterior aspects of the cortex loaded in net tension. As strain magnitudes increased through the step, the NA showed varying degrees of rotation among the individuals, but often became more closely aligned with the anatomical DV axis (Figs 2, 3). Although such a NA orientation would suggest prominent AP bending in the anatomical frame of reference, in the context of the axial rotation of the femur that occurs through the course of the stance phase in cooters, which tends to shift the anterior aspect of the femur to face ventrally in absolute space (Butcher and Blob, 2008), the NA orientations we observed are consistent with the maintenance of DV bending (in an absolute frame of reference) throughout the step as the femur rotates anteriorly. In addition, the displacement of the NA from the centroid and the extent of compressive strains across the femoral cross section confirm loading in axial compression, in addition to bending and torsion, for cooter femora. In one individual, planar analyses revealed strain distributions and orientations of the NA that differed from those of the other individuals, with the anterior aspect of the femur in compression and the posterior aspect in tension early in the step. However, in the last half of stance, strain distribution patterns for this individual closely resembled those of the other cooters; moreover, despite its differing strain distribution patterns, the plane of bone bending in this individual was maintained close to the anatomical DV axis (in an absolute frame of reference) through most of the step, as in the other cooters (Figs 2, 3).

Planar strain data indicate that peak tensile strains occur on the anterodorsal-to-anterior surfaces of the femur in cooters, and peak compressive strains at the posteroventral-to-posterior surfaces, rather than at the precise locations from which strains were recorded in the test animals by attached gauges. Because of this, actual peak strains in the cooter femur are generally higher than those recorded, averaging 43% higher across trials in which planar strain distributions were calculated (*N*=50 steps).

Femoral strain rates

Rates of axial strain (determined from the dorsal recording site) were variable but often reached quite high values, ranging from 943.5 με s^{-1} to 51 716.0 με s^{-1} across all sampled steps. Regression of strain magnitudes on corresponding strain rates for steps showed a strong positive relationship (r^2=0.636; P<0.001; Fig. 4), indicating that loading rates were quicker in steps with high strain magnitudes.

Bone mechanical properties and safety factors

Mean yield strains in bending for cooter femora (8316.0±1176.0 με; *N*=3) (Table 2) and tibiae (8785.6±2612.3 με; *N*=4) were similar, in contrast to the considerably higher yield stresses measured for femora *versus* tibiae (Butcher and Blob, 2008). These results suggest that cooter femora are stiffer than cooter tibiae. Both bones exhibited toughness in bending tests, with only one failing catastrophically. Femoral yield strains in torsion (9441.1±1805.7 με; *N*=3) were higher than those for bending (Table 2) and also moderately higher than values previously reported for bone from other species [8000 με (Currey, 1984)]. Each bone failed catastrophically in torsion.

Prior to safety factor calculations, peak functional bending and shear strains recorded from cooter femora during locomotor trials

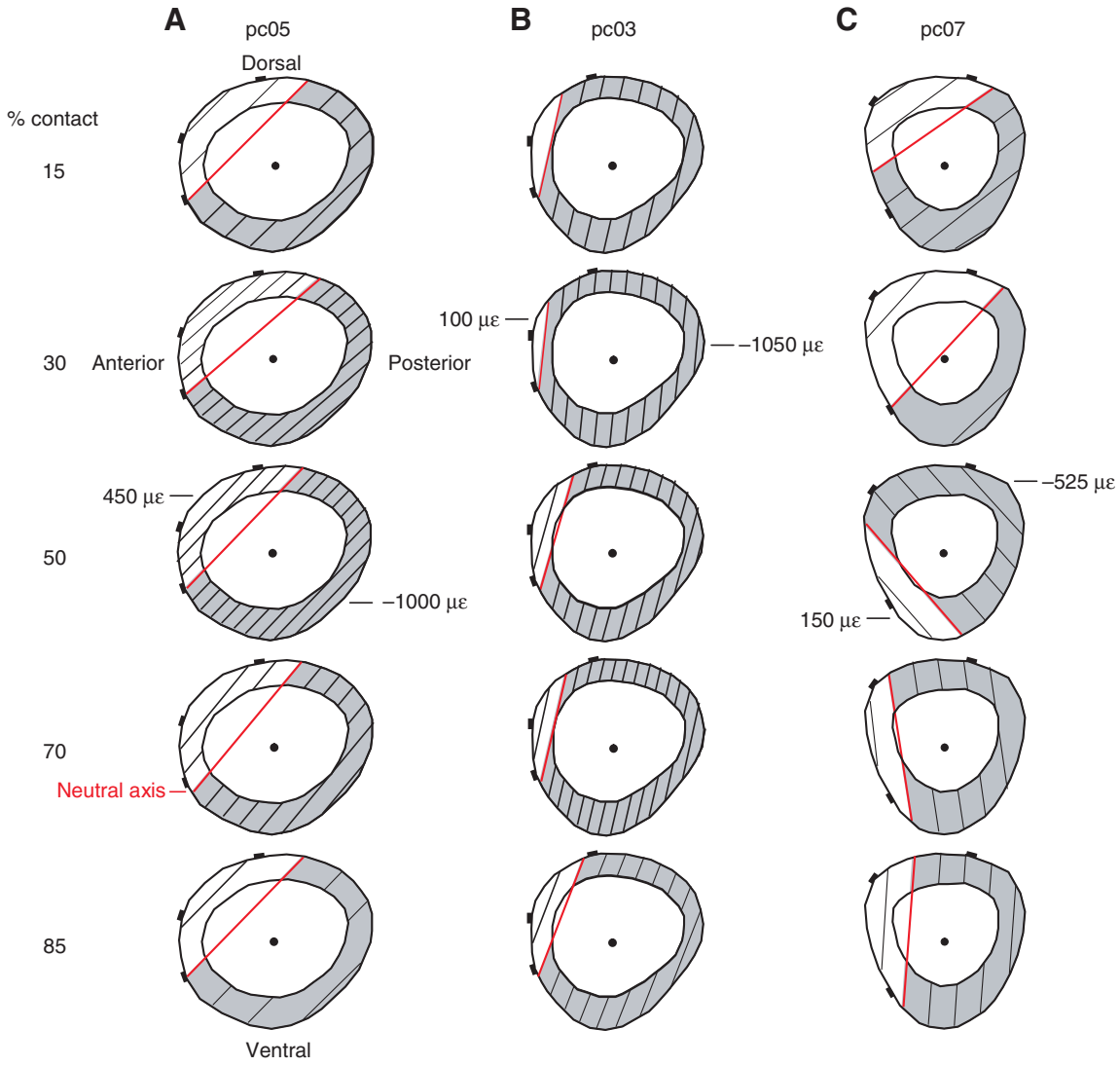

Fig. 3. Graphical comparisons of cross-sectional planar analyses of femoral strain distributions calculated for five time increments (% of contact) during representative walking for (A) individual pc05, (B) individual pc03 and (C) individual pc07. Time increments (% of contact) correspond to those plotted in Fig. 2. The centroid of each section is indicated by the black dot. Thin lines indicate contours of strain magnitude (all spaced at 100 με). Peak strains calculated for these steps are labeled on the sections at either 30% or 50% depending on the individual. Compressive strains are shaded gray. The neutral axis (NA) of bending (strain=0 με) is indicated by the red line (strain contour) separating compressive and tensile strains. Strain gauge locations are indicated by the black bars around the cortex of the femoral cross-sections. Anatomical directions are labeled in A and reflect the anatomical AP and DV axes illustrated in Fig. 2B.

Table 2. Mechanical properties, estimated actual peak strains and safety factors for the femur of *P. concinna*

Mechanical properties			Peak strains		Safety factors	
Yield strain bending (με)	Yield strain shear (με)	Proportional increase in strain	Calculated tensile bending (με)	Calculated shear (με)	Femur bending 'mean'	Femur shear 'mean'
8316.0±1176.0 (3)	9441.1±1805.7 (3)	1.43	1873.5	2718.9	4.4–6.9*	3.8

Mechanical property values are means (± s.d.); number of bones tested is in parentheses.
Peak strain estimates were calculated based on planar strain distributions; these provided a quantitative measure of the proportional increases in recorded strains (Table 1) used to determine estimated strains.
'Mean' safety factor calculations are described in the text.
*Low safety factor determined from highest individual mean value of principal strain; high safety factor determined as the grand 'mean' safety factor across *N*=4 turtles for which ROS data were available.

were multiplied by 1.43 to reflect results of planar strain analyses (see above) that showed peak strains could be 43% higher than measured strains. Based on data from the individual (pc04) that had the highest recorded principal strains on the anterior surface of the femur, an average value of 1873.5 με and maximum value of 2373.9 με for peak functional strain were calculated, producing a

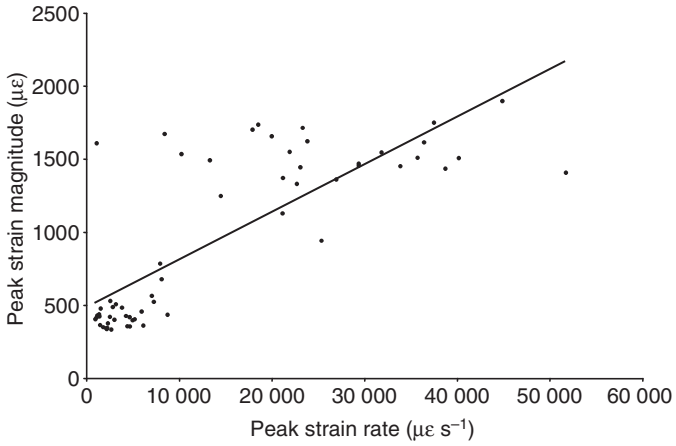

Fig. 4. Bivariate plot of strain magnitudes (in με) *versus* corresponding strain rates (in με s^{-1}) for N=60 individual steps from river cooter turtles. All data are plotted as absolute values. Solid line reflects a linear least-squares regression of the pooled data (y=0.0326x+479.86). There was a significant positive correlation between strain magnitude and strain rate (P<0.001, r^2=0.636).

mean safety factor of 4.4 and a worst-case estimate of 3.5 in bending (Table 2). However, if peak functional strains are derived from the grand mean of data for all turtles irrespective of the gauge location from which peak principal strains were recorded, an upper safety factor estimate of 6.9 in bending is derived (Table 2). Safety factors in shear were lower, with a mean safety factor estimate of 3.8 (based on the grand mean of peak shear strains across all turtles, regardless of recording site) and a worst-case estimate of 1.8 determined from the single highest magnitude of calculated peak shear strain, 5315.8 με, on the anterior surface of the femur (Table 2).

DISCUSSION

Femoral loading mechanics in river cooter turtles: correspondence between strain and force-platform data

The bone loading patterns we determined for terrestrial locomotion in cooters using direct measurements of *in vivo* strains were highly consistent with our previous conclusions derived from indirect bone stress evaluations based on force-platform studies (Butcher and Blob, 2008). For example, both strain and force-platform data gave similar indications of the timing of peak femoral loading (at 41.1±5.8% of contact for strain studies *versus* 36.6±3.2% in force-platform studies), which occurred on average prior to midstance in both analyses. Moreover, both stress and strain evaluations indicated that the cooter femur was subjected to a similar combination of loading regimes including bending, axial compression and torsion. Gauge recordings showed both tensile and compressive strains on the femoral cortex (Table 1, Fig. 1), supporting the presence of bending as inferred from calculations of stresses induced by the net GRF and muscle forces (Butcher and Blob, 2008). Planar strain analyses also showed that the NA was displaced from the cross-sectional centroid such that a greater portion of the femoral cortex was loaded in net compression, indicating (as seen in stress analyses) that, to support the weight of the body, axial compression is superimposed on bending in turtle femora. ROS gauge data further showed that principal strain orientations were close to 45° from the long axis of the femur, producing substantial shear strains and significant torsional loading, as suggested by calculations of the torsional moment of the GRF in force-platform studies (Butcher and Blob, 2008). Thus, major aspects of interpretations of load timing and regime are corroborated between our two experimental approaches.

Correspondence between the results of strain and force-platform analyses extended beyond these broad comparisons to more detailed aspects of femoral loading in cooters. For example, one unexpected result from our force-platform study was that femoral bending appeared to act about an axis that placed the anterodorsal aspect of the cortex in net tension and the posteroventral aspect of the femur in compression (Butcher and Blob, 2008). This differed from results in other non-avian reptiles (alligators and iguanas), in which the anteroventral aspect of the femur experienced net tension in bending (Blob and Biewener, 1999; Blob and Biewener, 2001). Planar strain analyses (Fig. 3) generally confirmed patterns determined from force-platform analyses, showing net tensile strains on the anterior-to-anterodorsal surfaces of the femur, rather than more ventral locations. The distinctive distribution of tension and compression in cooter femora, indicated by both stress and strain analyses, may reflect a greater degree of femoral axial rotation in turtles compared with other reptiles. In alligators and lizards, anterior (inward) axial rotation through the step might only bring the anatomical anterior aspect of the bone to face ventrally (i.e. towards the ground) in an absolute frame of reference (Blob and Biewener, 2001). However, greater axial rotation in turtles could bring the anatomical anterodorsal aspect of the femur to face toward the ground in an absolute frame of reference, where it would become the tensile surface of the bone in bending induced by the action of a nearly vertical net GRF (Butcher and Blob, 2008).

The significance of femoral torsion in cooters that was suggested by force-platform analyses was also confirmed by strain data. Shear strains calculated from ROS recordings showed peak values averaging near 1900 με across all gauge locations and exceeding 2900 με in one individual (Table 1). Peak shear strains were substantially higher than peak axial strains and 1.6–1.8 times higher than peak principal strain magnitudes for each individual and gauge location. The prominence of these shear strain magnitudes matches well with the high shear stresses estimated from force-platform analyses, in which only torsion induced by the GRF (without torsion induced by muscles) could be considered (Butcher and Blob, 2008). Verification of high torsional loading of the femur in turtles *via* our strain recordings is a further indication that dragging a large tail during locomotion may not be required to generate torsional limb bone loading in quadrupeds, (Willey et al., 2004; Reilly et al., 2005). In fact, shear strains reflecting torsion of the femur reach a maximum early in the step in cooters (Fig. 1), when the inward rotational moment of the GRF (Butcher and Blob, 2008) and the actions of limb muscles that could retract and inwardly rotate the femur (Blob et al., 2008) are likely acting in conjunction, potentially contributing to the high level of torsional loading.

Limb bone strains in turtles compared with other taxa

Strain data from cooters validate the conclusions of force-platform studies (Butcher and Blob, 2008) that femoral loading regimes and magnitudes are, generally, similar between turtles and other reptiles (Blob and Biewener, 1999; Blob and Biewener, 2001) during terrestrial locomotion. Although, as noted above, there are moderate differences in the orientation of femoral bending determined for cooters *versus* that determined in alligators and iguanas, the presence of substantial bending, axial compression and torsion as femoral loading regimes is indicated in all three lineages. Moreover, magnitudes of femoral axial compression and bending are comparable in all three groups. In both turtles (Fig. 3) and alligators (Blob and Biewener, 1999), planar strain analyses indicate that the

NA is displaced far from the cross-sectional centroid of the femur at the time of peak strain, demonstrating significant axial compression. Allowing for minor variation in gauge placement across individuals, measured axial strain magnitudes from comparable anatomical locations are also generally similar across the three species during high-exertion locomotion. For example, recorded tensile strains from gauges on the anterior surface of the femur averaged 218.9±118.2 με in cooters (Table 1) compared with 377±162 με in alligators and 288±130 με in iguanas for fast steps (Blob and Biewener, 1999). Although these mean values differ, their range of overlap is substantial, and the differences in these means are minor compared with their differences from the higher values typically recorded from birds and mammals (Biewener et al., 1983; Biewener, 1993; Lieberman et al., 2003; Main and Biewener, 2007). Peak compressive principal strains across our individual cooters averaged only –1082.2±424.9 με (Table 1), somewhat higher than values recorded previously from alligators and iguanas [generally <1000 με (Blob and Biewener, 1999)] but still considerably lower than values commonly reported for the limb bones of birds and mammals, which often approach or exceed 2000 με (Biewener, 1993; Carrano, 1998; Main and Biewener, 2007).

Similar to other non-avian reptiles (Blob and Biewener, 1999), femoral shear strains in cooters (Table 1) indicate considerably greater limb torsion in turtles than has been typically found in other lineages of quadrupedal tetrapods (e.g. Biewener, 1990; Main and Biewener, 2004). However, the high magnitudes of shear strains calculated for cooter femora (>1400 με, up to 2900 με in one individual) substantially exceed values previously calculated for alligators and iguanas [~1000–1100 με (Blob and Biewener, 1999)]. These results corroborate similar patterns of relative shear stress magnitudes in reptilian lineages calculated from force-platform analyses, in which cooter femora were found to have higher torsional stresses than other reptiles and, in fact, among the highest torsional limb bone stresses for terrestrial tetrapods (Blob and Biewener, 2001; Butcher and Blob, 2008). Both planar strain analyses (Fig. 3) and stress analyses (Butcher and Blob, 2008) suggest that cooters may rotate the femur about its long axis more than alligators or iguanas during terrestrial locomotion, a factor that might contribute to the elevation of torsional loads seen in turtles. A second factor that might contribute to high torsional loads in turtle limb bones is the rigidity of their body axis (Butcher and Blob, 2008). In other sprawling taxa, lateral undulations of the body axis might help to accommodate twisting of the femur; however, with the body axis (and thus, through the sacrum, the pelvis) fused to the shell in turtles, the femur would have to resist all such loads by itself.

In addition to turtles, alligators and lizards, elevated torsional loads have been observed in the hindlimb bones of birds during terrestrial locomotion (Biewener et al., 1986; Carrano, 1998; Main and Biewener, 2007). Because birds, as diapsid archosaurs, belong to the broader reptilian clade including turtles, crocodilians and lizards (Gauthier et al., 1988; Modesto and Anderson, 2004), it is possible that the torsion of hindlimb bones observed in birds reflects the retention of an ancestral condition in this lineage. However, it is not clear that hind limb torsion seen in birds and other reptiles results from similar underlying mechanical causes (Main and Biewener, 2007). Axial rotation of the femur induced by action of the caudofemoral muscles and the GRF has been cited as a primary proximate factor leading to torsional limb bone loading in quadrupedal reptiles (Blob and Biewener, 1999; Blob, 2000; Blob, 2001; Blob and Biewener, 2001; Reilly et al., 2005; Butcher and Blob, 2008). However, such rotation is not clearly evident in terrestrial birds (Main and Biewener, 2007). Given the distribution of lineages in which torsional limb bone loading has been observed during terrestrial locomotion, it is possible that it could be an ancestral feature of tetrapod locomotion originally related to sprawling limb posture. Bone loading data from additional outgroup lineages, such as amphibians, could provide insight into this possibility. However, with a different mechanical basis (i.e. without femoral axial rotation), torsional loading patterns seen in bird hindlimb bones might well have arisen independently from those seen in other non-avian reptiles through the course of functional changes from more immediate avian ancestors.

Although turtles are typically regarded as among the slowest of terrestrial tetrapods, the highest rates of bone loading we measured in cooters (~50 000 s^{-1}) approach and, in some cases, exceed values determined for the limb bones of other species during terrestrial locomotion [e.g. humans, 5000–22 000 s^{-1} (Burr et al., 1996); dog and horse, ~100 000 s^{-1} (Rubin and Lanyon, 1982)]. Moreover, as noted in studies of mammalian feeding (Ross et al., 2007), strain magnitude is strongly correlated with strain rate (Fig. 4), such that steps in which the femur experiences higher strains tend to be steps in which the limb is loaded more quickly. Bones loaded at higher strain rates can typically withstand greater strain magnitudes before yield failure (Currey, 1988; Courtney et al., 1994; Yeni and Fyhrie, 2003; Földhazy et al., 2005), so the correlation between loading rate and magnitude could help convey an improved ability of cooters to resist the highest loads their limb bones encounter. However, given the generally low magnitudes of axial strain seen in turtle femora and their high safety factors (Table 2, see below), the functional importance of such contributions is probably quite limited.

Safety factors in the turtle femur: comparisons and implications for the evolution of limb bone design

Strain-based 'mean' safety factors for the femur of river cooters ranged from 4.4 to 6.9 in bending and were evaluated at 3.8 in torsion (Table 2), values lower than those derived from force-platform data in bending (13.9), but slightly higher in shear (3.1) (Butcher and Blob, 2008) (Butcher and Blob, in press). Differences in safety factor calculations between *in vivo* strain and force-platform studies have been found in other taxa, including horses, alligators and iguanas (Biewener et al., 1983; Blob and Biewener, 1999; Blob and Biewener, 2001). However, in contrast to our results for turtle femora in bending, other comparisons of these methods tend to show force-platform studies producing higher estimates of limb bone loads and, thus, lower safety factors. Although we made a strong effort to model limb muscle activity in cooters as realistically as possible (Butcher and Blob, 2008), model inaccuracies [inappropriate assumptions about the action and orientation of limb muscles (Biewener et al., 1983; Blob and Biewener, 2001)] could lead to higher estimates of safety factors *via* either experimental method. In addition, differences in the method of eliciting locomotion from the study animals (in treadmill strain studies *versus* animals choosing their own speed in the force-platform trackway) might also contribute to differences in the load magnitudes resulting from each study.

Our strain-based evaluations of femoral safety factors for cooters are moderately lower than strain-based estimates previously calculated for alligator and iguana femora [6.3–10.8 in bending, 4.9–5.4 in shear (Blob and Biewener, 1999)] but still at least moderately higher than values of 2–4 [average 2.9 (Blob and Biewener, 1999)] typical for avian and mammalian limb bones (Alexander, 1981; Lanyon and Rubin, 1985; Biewener, 1993; Biewener and Dial, 1995). Thus, even accounting for differences in the estimates of femoral safety factors between our two experimental approaches, the femoral safety factors of turtles specifically, and non-avian reptiles more broadly, are generally higher than those of birds

and mammals. Differences in both load magnitudes and bone mechanical properties may contribute to the differing safety factors of these lineages. In addition to having lower bending strains in their limb bones than most birds and mammals (Table 1), cooter femora had higher tensile yield strains: 8316 με (Table 2), compared with mammalian and avian values between 5250 με and 6000 με (Currey, 1984; Biewener, 1993). Yield strains in bending for the femora of alligators and iguanas are also higher than those typical of birds and mammals (Blob and Biewener, 1999). In addition, even though high femoral shear strains were observed in turtles during locomotion (Table 1), yield strains in shear for cooter femora (9441 με) were higher than values typically attributed to non-reptilian taxa [8000 με (Currey, 1984)]. These data indicate that elevated mechanical resistance to failure may be a common factor contributing to the higher limb bone safety factors of non-avian reptiles compared with birds and mammals. Although variation in limb bone mechanical properties has not typically been viewed as a major factor contributing to the diversity of tetrapod limb bone designs and functional capacities (Biewener, 1982; Erickson et al., 2002), distinctive bone properties of some lineages have the potential to affect several aspects of limb performance (Blob and Snelgrove, 2006).

Confirmation, by our strain analyses, of the substantial femoral safety factors we observed in cooters based on force-platform data again raises questions as to why such a degree of protection against limb bone failure is found in turtles and the other quadrupedal reptiles in which bone loading has been evaluated. One potential advantage suggested for high limb bone safety factors in reptiles is that they could reduce the risk of fatigue failure (Carter et al., 1981) that might result from low bone remodeling rates (Enlow, 1969; de Ricqlès, 1975; de Ricqlès et al., 1991), which could limit the capacity for repair of microdamage resulting from cyclic loading in locomotion (Lanyon et al., 1982; Burr et al., 1985). While this might be the case in the limb bones of turtles, other species of non-avian reptiles with similar low rates of bone remodeling have been reported to have skull bones that experience high strains that would result in low safety factors [alligator mandible (Ross and Metzger, 2004)]. However, such bones experiencing high strains tend to be loaded less frequently than limb bones (Ross and Metzger, 2004). High limb bone safety factors could also help reptiles to accommodate variability in the loading demands they encounter (Alexander, 1981; Lowell, 1985; Blob and Biewener, 1999). These could stem from variation in the loads they experience [coefficients of variation in peak strain magnitudes for cooters averaged 34.4% *versus* <8% in birds and mammals (Biewener, 1991)], as well as potential variation in bone mechanical properties related to the absorption of endosteal bone from the femur during egg-laying, at least in females (Edgren, 1960; Suzuki, 1963; Wink and Elsey, 1986). Although elevated safety factors might be expected to be energetically costly to maintain, such costs might be a limited burden in lineages such as turtles and crocodilians, in which locomotor energetic economy (e.g. mechanical energy recovery) is generally not a significant factor in performance (Willey et al., 2004; Zani et al., 2005). Alternatively, high limb bone safety factors, resulting from 'excessively' robust femora, may simply be a consequence of providing adequate surface area for the attachment of sufficiently large locomotor muscles to power locomotion and resist the high muscle forces that can be imposed during sprawling locomotion (Butcher and Blob, 2008). Such a scenario would suggest that skeletal design in the limb may be substantially influenced by the demands imposed by muscle arrangement and performance (Hutchinson and Garcia, 2002; Hutchinson, 2004).

Considerations of the diversity of limb bone safety factors and designs in terms of their costs and benefits are typically framed in the context that natural selection should act against bone designs with safety factors that are inadequate or excessive (Alexander, 1981; Lanyon, 1991; Diamond and Hammond, 1992; Diamond, 1998). However, other factors beyond the action of natural selection may contribute to the diversity of limb bone safety factors observed across tetrapod taxa (Garland, 1998). For non-avian reptiles in particular, high limb bone safety factors might have resulted incidentally from selection on other traits (e.g. bone surface for muscle attachment) or simply have been retained from ancestral lineages (Lande and Arnold, 1983; Blob and Biewener, 1999). Limb bone loading data from amphibians could help clarify such questions about the phylogenetic history of factors affecting tetrapod limb bone design. Thus, although our evaluations of loading mechanics in turtle limb bones have extended understanding of the diversity of bone loading patterns and designs in tetrapods, understanding the evolutionary origins of that diversity will require further examination of bone loading in a wider functional and phylogenetic range of species.

We thank M. Pruette for help in construction of strain gauges, A. Rivera for help with figures, two anonymous reviewers for comments on the manuscript draft, and S. Gosnell, S. Hill, T. Maie, A. Rivera, G. Rivera and M. Wright for assistance with surgeries, experiments and animal care. J. DesJardins (Clemson Bioengineering) provided access to and generous assistance with mechanical testing equipment, D. Lieberman (Harvard) provided software for planar analysis of limb bone strains, and S. Bennett (South Carolina Department of Natural Resources) coordinated permission for field collection of turtles (SCDNR Scientific Collecting Permits 39-2004 and 39-2006). D. Lee (UNLV) gave insightful suggestions about the potential for axial rigidity in turtles to contribute to femoral torsion. Support by NSF (IOB-0517340) and the Clemson Department of Biological Sciences is gratefully acknowledged.

REFERENCES

Alexander, R. McN. (1974). The mechanics of a dog jumping, *Canis familiaris*. *J. Zool. (Lond.)* **173**, 549-573.
Alexander, R. McN. (1981). Factors of safety in the structure of animals. *Sci. Prog.* **67**, 109-130.
Ashley-Ross, M. A. (1994a). Metamorphic and speed effects on hindlimb kinematics during terrestrial locomotion in the salamander *Dicamptodon tenebrosus*. *J. Exp. Biol.* **193**, 285-305.
Ashley-Ross, M. A. (1994b). Hindlimb kinematics during terrestrial locomotion in a salamander (*Dicamptodon tenebrosus*). *J. Exp. Biol.* **193**, 255-283.
Ashley-Ross, M. A. (1995). Patterns of hindlimb motor output during walking in the salamander *Dicamptodon tenebrosus*, with comparisons to other tetrapods. *J. Comp. Physiol. A* **177**, 273-285.
Bertram, J. E. and Biewener, A. A. (1988). Bone curvature: sacrificing strength for load predictability? *J. Theor. Biol.* **131**, 75-92.
Biewener, A. A. (1982). Bone strength in small mammals and bipedal birds: do safety factors change with body size? *J. Exp. Biol.* **98**, 289-301.
Biewener, A. A. (1983a). Locomotory stresses in the limb bones of two small mammals: the ground squirrel and chipmunk. *J. Exp. Biol.* **103**, 131-154.
Biewener, A. A. (1983b). Allometry of quadrupedal locomotion: the scaling of duty factor, bone curvature and limb orientation to body size. *J. Exp. Biol.* **105**, 147-171.
Biewener, A. A. (1989). Scaling body support in mammals: limb posture and muscle mechanics. *Science* **245**, 45-48.
Biewener, A. A. (1990). Biomechanics of mammalian terrestrial locomotion. *Science* **250**, 1097-1103.
Biewener, A. A. (1991). Musculoskeletal design in relation to body size. *J. Biomech.* **24 (Suppl 1),** 19-29.
Biewener, A. A. (1992). *In vivo* measurement of bone strain and tendon force. In *Biomechanics – Structures and Systems: A Practical Approach* (ed. A. A. Biewener), pp. 123-147. New York: Oxford University Press.
Biewener, A. A. (1993). Safety factors in bone strength. *Calcif. Tissue Int. (Suppl. 1).* **53,** S68-S74.
Biewener, A. A. and Dial, K. P. (1995). *In vivo* strain in the humerus of pigeons (*Columba livia*) during flight. *J. Morphol.* **225**, 61-75.
Biewener, A. A. and Full, R. J. (1992). Force platform and kinematic analysis. In *Biomechanics – Structures and Systems: A Practical Approach* (ed. A. A. Biewener), pp. 45-73. New York: Oxford University Press.
Biewener, A. A. and Taylor, C. R. (1986). Bone strain: a determinant of gait and speed? *J. Exp. Biol.* **123**, 383-400.
Biewener, A. A., Thomason, J. J., Goodship, A. and Lanyon, L. E. (1983). Bone stress in the horse forelimb during locomotion at different gaits: a comparison of two experimental methods. *J. Biomech.* **16**, 565-576.
Biewener, A. A., Swartz, S. M. and Bertram, J. E. A. (1986). Bone modeling during growth: dynamic strain equilibrium in the chick tibiotarsus. *Calcif. Tissue Int.* **39**, 390-395.
Biewener, A. A., Thomason, J. J. and Lanyon, L. E. (1988). Mechanics of locomotion and jumping in the horse (*Equus*): *in vivo* stress in the tibia and metatarsus. *J. Zool. (Lond.)* **214**, 547-565.

Blob, R. W. (2000). Interspecific scaling of the hindlimb skeleton in lizards, crocodilians, felids and canids: does limb bone shape correlate with limb posture? *J. Zool. (Lond.)* **250**, 507-531.
Blob, R. W. (2001). Evolution of hindlimb posture in non-mammalian therapsids: biomechanical tests of paleontological hypotheses. *Paleobiology* **27**, 14-38.
Blob, R. W. and Biewener, A. A. (1999). *In vivo* locomotor strain in the hindlimb bones of *Alligator mississippiensis* and *Iguana iguana*: implications for the evolution of limb bone safety factor and non-sprawling limb posture. *J. Exp. Biol.* **202**, 1023-1046.
Blob, R. W. and Biewener, A. A. (2001). Mechanics of limb bone loading during terrestrial locomotion in the green iguana (*Iguana iguana*) and American alligator (*Alligator mississippiensis*). *J. Exp. Biol.* **204**, 1099-1122.
Blob, R. W. and Snelgrove, J. M. (2006). Antler stiffness in moose (*Alces alces*): correlated evolution of bone function and material properties? *J. Morphol.* **267**, 1075-1086.
Blob, R. W., Rivera, A. R. V. and Westneat, M. W. (2008). Hindlimb function in turtle locomotion: limb movements and muscular activation across taxa, environment, and ontogeny. In *Biology of Turtles* (ed. J. Wyneken, M. H. Godfrey and V. Bels), pp. 139-162. Boca Raton: CRC Press.
Brinkman, D. (1980). The hindlimb step cycle of *Caiman sclerops* and the mechanics of the crocodile tarsus and metatarsus. *Can. J. Zool.* **58**, 2187-2200.
Brinkman, D. (1981). The hind limb cycle of *Iguana* and primitive reptiles. *J. Zool. (Lond.)* **181**, 91-103.
Burr, D. B., Martin, R. B., Schaffer, M. B. and Radin, E. L. (1985). Bone remodeling in response to *in vivo* fatigue microdamage. *J. Biomech.* **18**, 189-200.
Burr, D. B., Milgrom, C., Fyhrie, D. P., Forwood, M., Nyska, M., Finestone, A., Hoshaw, S., Saiag, E. and Simkin, A. (1996). *In vivo* measurement of human tibial strains during vigorous activity. *Bone* **18**, 405-410.
Butcher, M. T. and Blob, R. W. (2008). Mechanics of limb bone loading during terrestrial locomotion in river cooter turtles (*Pseudemys concinna*). *J. Exp. Biol.* **211**, 1187-1202.
Butcher, M. T. and Blob, R. W. (in press). Corrigendum. Mechanics of limb bone loading during terrestrial locomotion in river cooter turtles (*Pseudemys concinna*). *J. Exp. Biol.* **211**, 2369.
Carrano, M. T. (1998). Locomotion of non-avian dinosaurs: integrating data from hindlimb kinematics, *in vivo* strains and bone morphology. *Paleobiology* **24**, 450-469.
Carter, D. R. (1978). Anisotropic analysis of strain rosette information from cortical bone. *J. Biomech.* **11**, 199-202.
Carter, D. R., Harris, W. H., Vasu, R. and Caler, W. E. (1981). The mechanical and biological response of cortical bone to *in vivo* strain histories. In *Mechanical Properties of Bone*. AMD vol. 45 (ed. S. C. Cowin), pp. 81-92. New York: American Society of Mechanical Engineers.
Cirilo, S. R., Hill, S., Espinoza, N. R. and Blob, R. W. (2005). Limb bone strain rates in divergent locomotor modes: turtles and frogs compared. *Int. Comp. Biol.* **45**, 1119.
Claussen, D. L., Snashall, J. and Barden, C. (2004). Effects of slope, substrate, and temperature on forces associated with locomotion of the ornate box turtle, *Terrapene ornata*. *Comp. Biochem. Physiol.* **138A**, 269-276.
Courtney, A. C., Wachtel, E. F., Myers, E. R. and Hayes, W. C. (1994). Effects of loading rate on strength of the proximal femur. *Calcif. Tissue Int.* **55**, 53-58.
Currey, J. D. (1984). *The Mechanical Adaptations of Bones*. Princeton, NJ: Princeton University Press.
Currey, J. D. (1988). Strain rate and mineral content in fracture models of bone. *J. Orthop. Res.* **6**, 32-38.
Currey, J. D. (1990). Physical characteristics affecting the tensile failure properties of compact bone. *J. Biomech.* **23**, 837-844.
Currey, J. D. (2002). *Bones. Structure and Mechanics*. Princeton, NJ: Princeton University Press.
Dally, J. W. and Riley, W. F. (1978). *Experimental Strain Analysis*. New York: McGraw-Hill.
Davies, H. M. S., McCarthy, R. N. and Jeffcott, L. B. (1993). Surface strain on the dorsal metacarpus of Thoroughbreds at different speeds and gaits. *Acta Anat. (Basel)* **146**, 148-153.
Demes, B., Qin, Y. X., Stern, J. T., Larson, S. G. and Rubin, C. T. (2001). Patterns of strain in the macaque tibia during functional activity. *Am. J. Phys. Anthropol.* **116**, 257-265.
de Margerie, E., Sanchez, S., Cubo, J. and Castenet, J. (2005). Torsional resistance as a principal component of the structural design of long bones: comparative multivariate evidence in birds. *Anat. Rec. A. Discov. Mol. Cell. Evol. Biol.* **282**, 49-66.
de Ricqlès, A. J. (1975). On bone histology of living and fossil reptiles, with comments on its functional and evolutionary significance. In *Morphology and Biology of Reptiles.* Linnean Society Symposium Series, Number 3 (ed. A. d' A. Bellairs and C. B. Cox) pp. 123-150. New York: Academic Press.
de Ricqlès, A. J., Meunier, F. J., Castanet, J. and Francillon-Vieillot, H. (1991). Comparative microstructure of bone. In *Bone: Bone Matrix and Bone Specific Products*. Vol. 3 (ed. B. K. Hall), pp. 1-78. Baca Raton: CRC Press.
Diamond, J. M. (1998). Evolution of biological safety factors: a cost/benefit analysis. In *Principles of Animal Design* (ed. D. W. Weibel, C. R. Taylor and L. Bolis), pp. 21-27. Cambridge: Cambridge University Press.
Diamond, J. M. and Hammond, K. A. (1992). The matches, achieved by natural selection, between biological capacities and their natural loads. *Experientia* **48**, 551-557.
Edgren, R. A. (1960). A seasonal change in bone density in female musk turtles, *Sternothaerus odoratus* (Latreille). *Comp. Biochem. Physiol.* **1**, 213-217.
Enlow, D. H. (1969). The bones of reptiles. In *Biology of the Reptilia, I, Morphology A* (ed. C. Gans, A. d' A. Bellairs and T. S. Parsons), pp. 45-80. London: Academic Press.
Erickson, G. M., Catanese, J. III. and Keaveny, T. M. (2002). Evolution of the biomechanical material properties of the femur. *Anat. Rec.* **268**, 115-124.
Földhazy, Z., Arndt, A., Milgrom, C., Finestone, A. and Ekenman, I. (2005). Exercise-induced strain and strain rate in the distal radius. *J. Bone Joint Surg.* **87B,** 261-266.
Furman, B. R. and Saha, S. (2000). Torsional testing of bone. In *Mechanical Testing of Bone and the Bone-Implant Interface* (ed. Y. H. An and R. A. Draughn), pp. 219-239. Boca Raton: CRC Press.
Garland, T. Jr. (1998). Conceptual and methodological issues in testing the predictions of symmorphosis. In *Principles of Animal Design* (ed. D. W. Weibel, C. R. Taylor and L. Bolis), pp. 40-47. Cambridge: Cambridge University Press.
Gatesy, S. M. (1991). Hindlimb movements of the American alligator (*Alligator mississippiensis*) and postural grades. *J. Zool. (Lond.)* **224**, 577-588.
Gatesy, S. M. (1999). Guineafowl hind limb function I: cineradiographic analysis and speed effects. *J. Morphol.* **240**, 127-142.
Gauthier, J., Kluge, A. G. and Rowe, T. (1988). The early evolution of the Amniota. In *The Phylogeny and Classification of the Tetrapods*. Vol. 1 (ed. M. J. Benton), pp. 103-155. Oxford: Clarendon Press.
Hutchinson, J. R. (2004). Biomechanical modeling and sensitivity analysis of bipedal running ability. I. Extant taxa. *J. Morphol.* **262**, 421-440.
Hutchinson, J. R. and Garcia, M. (2002). *Tyrannosaurus* was not a fast runner. *Nature* **415**, 1018-1021.
Jayes, A. S. and Alexander, R. McN. (1980). The gaits of chelonians: walking techniques for very slow speeds. *J. Zool. (Lond.)* **191**, 353-378.
Jenkins, F. A. (1971). Limb posture and locomotion in the Virginia opossum (*Didelphis marsupialis*) and in other cursorial mammals. *J. Zool. (Lond.)* **165**, 303-315.
Keller, T. S. and Spengler, D. M. (1989). Regulation of bone stress and strain in the immature and mature rat femur. *J. Biomech.* **22**, 1115-1127.
Lande, R. and Arnold, S. J. (1983). The measurement of selection on correlated characters. *Evolution* **37**, 1210-1226.
Lanyon, L. E. (1991). Biomechanical properties of bone and response of bone to mechanical stimuli: functional strain as a controlling influence on bone modeling and remodeling behavior. In *Bone: Bone Matrix and Bone Specific Products*. Vol. 3 (ed. B. K. Hall) pp. 79-108. Boca Raton: CRC Press.
Lanyon, L. E. and Rubin, C. T. (1985). Functional adaptation in skeletal structures. In *Functional Vertebrate Morphology* (ed. M. Hildebrand, D. M. Bramble, K. F. Liem and D. B. Wake), pp. 1-25. Cambridge: The Belknap Press.
Lanyon, L. E., Goodship, A. E., Pye, C. J. and MacFie, J. H. (1982). Mechanically adaptive bone remodeling. *J. Biomech.* **15**, 141-154.
Lieberman, D. E., Pearson, O. M., Polk, J. D., Demes, B. and Crompton, A. W. (2003). Optimization of bone growth and remodeling in response to loading in tapered mammalian limbs. *J. Exp. Biol.* **206**, 3125-3138.
Lieberman, D. E., Polk, J. D. and Demes, B. (2004). Predicting long bone loading from cross-sectional geometry. *Am. J. Phys. Anthropol.* **123**, 156-171.
Lowell, R. B. (1985). Selection for increased safety factors of biological structures as environmental unpredictability increases. *Science* **228**, 1009-1011.
Main, R. P. and Biewener, A. A. (2004). Ontogenetic patterns of limb loading, *in vivo* strains and growth in the goat radius. *J. Exp. Biol.* **207**, 2577-2588.
Main, R. P. and Biewener, A. A. (2007). Skeletal strain patterns and growth in the emu hindlimb during ontogeny. *J. Exp. Biol.* **210**, 2676-2690.
Modesto, S. P. and Anderson, J. S. (2004). The phylogenetic definition of Reptilia. *Syst. Biol.* **53**, 815-821.
Nunamaker, D. M., Butterweck, D. M. and Provost, M. T. (1990). Fatigue fractures in Thoroughbred racehorses: relationships between age, peak bone strain, and training. *J. Orthop. Res.* **8**, 604-611.
Reilly, S. M. (2000). Locomotion in the quail (*Coturnix japonica*): the kinematics of walking and increasing speed. *J. Morphol.* **243**, 173-185.
Reilly, S. M. and Elias, J. A. (1998). Locomotion in *Alligator mississippiensis*: kinematic effects of speed and posture and their relevance to the sprawling-to-erect paradigm. *J. Exp. Biol.* **201**, 2559-2574.
Reilly, S. M., Willey, J. S., Biknevicius, A. R. and Blob, R. W. (2005). Hindlimb function in the alligator: integrating movements, motor patterns, ground reaction forces and bone strain of terrestrial locomotion. *J. Exp. Biol.* **208**, 993-1009.
Romer, A. S. (1956). *Osteology of the Reptiles*. Chicago: University of Chicago Press.
Ross, C. F. and Metzger, K. A. (2004). Bone strain gradients and optimization in vertebrate skulls. *Ann. Anat.* **186**, 387-396.
Ross, C. F., Dharia, R., Herring, S. W., Hylander, W. L., Liu, Z. J., Rafferty, K. L., Ravosa, M. J. and Williams, S. H. (2007). Modulation of mandibular loading and bite force in mammals during mastication. *J. Exp. Biol.* **210**, 1046-1063.
Rubin, C. T. and Lanyon, L. E. (1982). Limb mechanics as a function of speed and gait: a study of functional strains in the radius and tibia of horse and dog. *J. Exp. Biol.* **101**, 187-211.
Suzuki, H. K. (1963). Studies on the osseous system of the slider turtle. *Ann. N. Y. Acad. Sci.* **109**, 351-410.
Walker, W. F. Jr. (1971). A structural and functional analysis of walking in the turtle, *Chrysemys picta marginata*. *J. Morph.* **134**, 195-214.
Walker, W. F. Jr. (1973). Locomotor apparatus of Testudines. In *Biology of the Reptilia*: *Morphology D*. Vol. 4 (ed. C. Gans and T. S. Parsons), pp. 1-100. London: Academic Press.
Willey, J. S. and Blob, R. W. (2004). Tail kinematics of juvenile common snapping turtles during aquatic walking. *J. Herpetol.* **38**, 360-369.
Willey, J. S., Biknevicius, A. R., Reilly, S. M. and Earls, K. D. (2004). The tale of the tail: limb function and locomotor mechanics in *Alligator mississippiensis*. *J. Exp. Biol.* **207**, 553-563.
Wink, C. S. and Elsey, R. M. (1986). Changes in femoral morphology during egg-laying in *Alligator mississippiensis*. *J. Morphol.* **189**, 183-188.
Yeni, Y. N. and Fyhrie, D. P. (2003). A rate-dependent microcrack-bridging model that can explain the strain rate dependency of cortical bone apparent yield strength. *J. Biomech.* **36**, 1343-1353.
Zani, P. A., Gottschall, J. S. and Kram, R. (2005). Giant Galápagos tortoises walk without inverted pendulum mechanical-energy exchange. *J. Exp. Biol.* **208**, 1489-1494.
Zug, G. R. (1971). Buoyancy, locomotion, morphology of the pelvic girdle and hindlimb, and systematics of cryptodiran turtles. *Occas. Pap. Mus. Zool. Univ. Mich.* **142**, 1-98.